



Novel Potent 5-HT₃ Receptor Ligands Based on the Pyrrolidone Structure. Effects of the Quaternization of the Basic Nitrogen on the Interaction with 5-HT₃ Receptor

Andrea Cappelli,^{a,*} Andrea Gallelli,^a Carlo Braile,^a Maurizio Anzini,^a
Salvatore Vomero,^a Laura Mennuni,^b Francesco Makovec,^b M. Cristina Menziani,^c
Pier G. De Benedetti,^c Alessandro Donati^d and Gianluca Giorgi^c

^aDipartimento Farmaco Chimico Tecnologico, Università degli Studi di Siena, Via A. Moro, 53100 Siena, Italy

^bRotta Research Laboratorium S.p.A., Via Valosa di Sopra 7, 20052 Monza, Italy

^cDipartimento di Chimica, Università degli Studi di Modena e Reggio Emilia, Via Campi 183, 41100 Modena, Italy

^dDipartimento di Scienze e Tecnologie Chimiche e dei Biosistemi, Università degli Studi di Siena, Via A. Moro, 53100 Siena, Italy

^eCentro Interdipartimentale di Analisi e Determinazioni Strutturali, Università degli Studi di Siena, Via A. Moro, 53100 Siena, Italy

Received 6 December 2001; accepted 8 March 2002

Abstract—The results of a comprehensive structure–affinity relationship study on the effect of the quaternization (i.e., *N*-methylation) of structurally different ligands in the classes of tropane and quinuclidine derivatives are described. This study shows that the effects of the quaternization of the basic nitrogen of these 5-HT₃ receptor ligands appear to be strictly structure-dependent suggesting that different binding modes are operative at 5-HT₃ receptor binding site. The different effect of the quaternization of the basic nitrogen of structurally different ligands were rationalized in terms of the interaction with the receptor by means of the combined use of experimental techniques (X-ray diffraction and NMR studies) and computational simulation studies. © 2002 Elsevier Science Ltd. All rights reserved.

Introduction

Within the context of serotonin (5-hydroxytryptamine, 5-HT) receptor subtypes, 5-HT₃ receptor represents a special case because it is a ligand-gated ion channel¹ (LGIC) exhibiting the pentameric structure characteristic of other ligand-gated ion channels such as nicotinic acetylcholine (nACh), glycine, and γ -aminobutyric acid type A (GABA_A) receptors.²

The development of selective 5-HT₃ receptor antagonists has received a great interest in recent years and the therapeutic role of ondansetron (**1**), granisetron (BRL 43694, **2**), and tropisetron (ICS 205-930, **3**) as antiemetic drugs has been established clearly. Moreover, preclinical studies suggested that 5-HT₃ receptor antagonists might be clinically useful in a number of situations: depressive, cognitive, and psychotic disorders, drug and alcohol abuse, treatment of pain and irritable bowel syndrome.³

At an earlier stage our group was involved in the development of arylpiperazine 5-HT₃ receptor ligands **4**,⁴ while more recently our attention was focused on conformationally constrained derivatives of the classical 5-HT₃ receptor antagonists. Indeed, in a recent paper we reported the synthesis and pharmacological characterization of a new class of potent 5-HT₃ receptor ligands based on the pyrrolidone structure and containing the tropane and quinuclidine moieties **5–7**. By means of the integration of a classical medicinal chemistry approach [based on extensive qualitative structure–affinity relationship (SAFIR) studies] with a computational approach (receptor mapping, homologue modelling and docking simulation) we obtained a picture of the complexity of the ligand–receptor interaction.⁵

The basic assumption of the proposed binding paradigm is that the positively charged nitrogen of the ligands plays a key role in both the receptor recognition (long range interaction) and the docking process (ionic and/or charge reinforced hydrogen bonding interactions). However, experimental evidence concerning the different effect of the quaternization of the basic nitrogen of structurally

*Corresponding author. Tel.: +39-0577-234-320; fax: +39-0577-234-333; e-mail: cappelli@unisi.it

different ligands suggests that the charged nitrogen interacts with the receptor with different modalities: different amino acid counterparts or different orientations when structurally dissimilar ligands are considered.⁶ Thus, this paper describes the results of a comprehensive SAFIR study on the effect of the quaternization (i.e., *N*-methylation) of structurally different ligands in the classes of tropane and quinuclidine derivatives. The different effects of the quaternization of the basic nitrogen of structurally different ligands were rationalized in terms of the interaction with the receptor by means of the combined use of experimental techniques (X-ray diffraction and NMR studies) and computational simulation studies.

Chemistry

Tropane derivatives **5a**, **6a**, and **7a** and the enantiomers of quinuclidine derivatives **5d**, **6c,e**, and **7c** were prepared as described in the previous paper.⁵ Quaternary derivatives **5c,e**, **6b,d,f**, and **7b,d** were prepared by reaction of the corresponding free bases **5a,d**, **6a,c,e**, and **7a,c** with methyl iodide in methanol at room temperature.

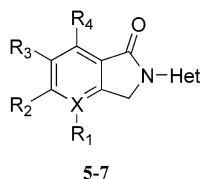
Results

Binding studies

The newly synthesized compounds were tested for their potential ability to displace [³H]granisetron specifically bound to 5-HT₃ receptor in rat cortical membranes.⁷ The results of the binding studies are summarized in Table 1.

The comparison of the affinity of the quaternary compounds with that shown by the corresponding free bases (which are protonated at physiological pH) shows that the effects of the quaternization of the basic nitrogen of 5-HT₃ receptor ligands is strictly structure-dependent. In fact, the dimethyl quaternary tropane derivative **5c** shows an affinity indistinguishable from those shown by the corresponding monomethyl derivative **5a** and the nortropane derivative **5b**, while quaternary compound **6b** is 2 times less potent than the corresponding monomethyl derivative **6a**, and quaternary derivative **7b** is 5 times less potent than the corresponding monomethyl derivative **7a**. Therefore in the small subclass of tropane ligands, the effects of the quaternization appear to be affected by the geometry of the heteroaromatic moiety.

Table 1. Binding affinities for the central 5-HT₃ receptor and effects on [¹⁴C]guanidium accumulation in NG 108-15 cells of compounds **5–7**



Compd	Het	X	R ₁	R ₂	R ₃	R ₄	K _i (nM) ± SEM ^a	Intrinsic efficacy ^b
5a	<i>endo</i> -Tropan-3-yl ^c	C	H	H	–C ₄ H ₄ –		1.2 ± 0.23	Ant
5b	<i>endo</i> -Nortropan-3-yl ^d	C	H	H	–C ₄ H ₄ –		1.3 ± 0.47	
5c	<i>endo</i> -Tropan-3-yl(CH ₃ I) ^e	C	H		–C ₄ H ₄ –		1.0 ± 0.17	
(<i>S</i>)- 5d	(<i>S</i>)-Quinuclidin-3-yl ^f	C	H	H	–C ₄ H ₄ –		0.34 ± 0.09	Ant
(<i>R</i>)- 5d	(<i>R</i>)-Quinuclidin-3-yl	C	H	H	–C ₄ H ₄ –		1.8 ± 0.49	PA
(<i>S</i>)- 5e	(<i>S</i>)-Quinuclidin-3-yl(CH ₃ I) ^g	C	H	H	–C ₄ H ₄ –		20 ± 6.7	
(<i>R</i>)- 5e	(<i>R</i>)-Quinuclidin-3-yl(CH ₃ I)	C	H	H	–C ₄ H ₄ –		3.6 ± 1.2	
6a	<i>endo</i> -Tropan-3-yl	C	H	–C ₄ H ₄ –		H	52 ± 23	
6b	<i>endo</i> -Tropan-3-yl(CH ₃ I)	C		–C ₄ H ₄ –		H	104 ± 27	
(<i>S</i>)- 6c	(<i>S</i>)-Quinuclidin-3-yl	C	H	–C ₄ H ₄ –		H	31 ± 7.9	PA
(<i>R</i>)- 6c	(<i>R</i>)-Quinuclidin-3-yl	C	H	–C ₄ H ₄ –		H	3.8 ± 1.9	PA
(<i>S</i>)- 6d	(<i>S</i>)-Quinuclidin-3-yl(CH ₃ I)	C	H	–C ₄ H ₄ –		H	730 ± 240	
(<i>R</i>)- 6d	(<i>R</i>)-Quinuclidin-3-yl(CH ₃ I)	C	H	–C ₄ H ₄ –		H	69 ± 12	
(<i>S</i>)- 6e	(<i>S</i>)-Quinuclidin-3-yl	N		–C ₄ H ₄ –		H	87 ± 17	
(<i>R</i>)- 6e	(<i>R</i>)-Quinuclidin-3-yl	N		–C ₄ H ₄ –		H	0.83 ± 0.30	PA
(<i>S</i>)- 6f	(<i>S</i>)-Quinuclidin-3-yl(CH ₃ I)	N		–C ₄ H ₄ –		H	550 ± 190	
(<i>R</i>)- 6f	(<i>R</i>)-Quinuclidin-3-yl(CH ₃ I)	N		–C ₄ H ₄ –		H	230 ± 110	
7a	<i>endo</i> -Tropan-3-yl	C	–C ₄ H ₄ –		H	H	4.9 ± 0.50	Ant
7b	<i>endo</i> -Tropan-3-yl(CH ₃ I)	C	–C ₄ H ₄ –			H	25 ± 4.9	
(<i>S</i>)- 7c	(<i>S</i>)-Quinuclidin-3-yl	C	–C ₄ H ₄ –		H	H	6.0 ± 0.80	Ant
(<i>R</i>)- 7c	(<i>R</i>)-Quinuclidin-3-yl	C	–C ₄ H ₄ –		H	H	6.6 ± 1.5	A
(<i>S</i>)- 7d	(<i>S</i>)-Quinuclidin-3-yl(CH ₃ I)	C	–C ₄ H ₄ –		H	H	480 ± 160	
(<i>R</i>)- 7d	(<i>R</i>)-Quinuclidin-3-yl(CH ₃ I)	C	–C ₄ H ₄ –		H	H	670 ± 340	
2							0.35 ± 0.06	
5-HT							120 ± 34	

^aEach value is the mean ± SEM of three determinations and represents the concentration giving half the maximum inhibition of [³H]granisetron specific binding to rat cortical membranes.

^bA = pure agonist; PA = partial agonist; Ant = pure antagonist (see ref 5).

^cTropan-3-yl: 8-methyl-8-azabicyclo[3.2.1]oct-3-yl.

^dNortropan-3-yl: 8-azabicyclo[3.2.1]oct-3-yl.

^eTropan-3-yl(CH₃I): 8,8-dimethyl-8-azoniabicyclo[3.2.1]oct-3-yl.

^fQuinuclidin-3-yl: 1-azabicyclo[2.2.2]oct-3-yl.

^gQuinuclidin-3-yl(CH₃I): 1-methyl-1-azoniabicyclo[2.2.2]oct-3-yl.

On the other hand, preliminary study on the enantiomers of quinuclidine derivative **5d** revealed different effects depending on the configuration at the chiral center. Indeed, quaternization reduces the 5-HT₃ receptor affinity of the eutomer (*S*)-**5d** [cf., (*S*)-**5d** vs (*S*)-**5e**] and leaves that of the distomer (*R*)-**5e** practically unaltered. It is noteworthy that the enantiomers of quinuclidine derivative **5d** showed different intrinsic efficacies (see Table 1). This intriguing result stimulated a more detailed analysis of the effect of the quaternization in the quinuclidine derivative series. The study revealed a very complex behavior in which the configuration at the chiral center and the structural features of the heteroaromatic moiety may both play a role. For example, quaternization of the enantiomers of **6c** (both partial agonists) has the same effect of about 20-fold reducing the affinity on both the enantiomeric forms, while in the closely related compound **6e** the effect of the quaternization appears to be affected by the configuration of the chiral center as in the case of **5d**.

By ways of comparison, quaternary arylpiperazine derivative **4b** was almost two orders of magnitude less potent than the corresponding monomethyl free base **4a**.^{4c}

Structural studies

The quaternization of the basic nitrogen of the 5-HT₃ ligands studied is an apparently simple structural alteration, which, however, can modify several structural parameters. Among them, the conformational preferences are of special interest because the interaction of a ligand with its receptor might require a certain conformation, the so-called 'bioactive conformation'.

The azabicyclic system of quinuclidine derivatives studied is rigid and these compounds show only a degree of conformational freedom which is not (or is only marginally) affected by the quaternization of quinuclidine nitrogen. On the other hand, the tropane derivatives studied show in principle three types of conformational freedom: (a) rotation around the single bond attachment of the tropane moiety to the fused pyrrolidone nucleus, (b) the conformational flexibility of piperidine ring of the tropane moiety, and (c) pyramidal inversion of the tertiary amine nitrogen. Among them, (b) and (c) are affected by quaternization of the tropane nitrogen. For these reasons the structure of tropane derivatives was investigated by means of X-ray diffraction and NMR techniques.

Single crystal X-ray diffraction studies. The crystal structures of **5a** and **7a** are showed in Figures 1 and 2, respectively. The asymmetric unit of **7a** is formed by one molecule, while the one of **5a** is formed by two independent molecules.

The benz[*e*]isoindolone moiety is planar in both compounds. However, the presence of the carbonyl group at position 1, as it occurs in **5a**, causes larger deviations from the planarity with respect to those observed when the carbonyl is at position 3 as in compound **7a**. In fact, in one molecule of **5a**, C-3 and C-7 deviate −0.068 and −0.045 Å, respectively, from the least-squares plane,

while in the other molecule of **5a**, N-2A and C-6A show the largest deviations (0.065 and 0.062 Å, respectively) and, in the benz[*e*]isoindolone moiety of **7a**, N-2 shows the largest deviation (0.022 Å). The dihedral angles between the least-squares planes defined by the benz[*e*]isoindolone moiety and by the tropane piperidine ring are equal to 79.26 and 83.66° in the two molecules of **5a**, and 85.75° in **7a**.

The benz[*e*]isoindolone moiety is bound to the piperidine ring of the tropane at the equatorial position. The bond between N-2 and C-3' is oriented in such a manner that H-3' is in a *syn* position with respect to the pyrrolidone carbonyl suggesting the existence of an intramolecular interaction between H-3' and O-1 of **5a**. This alignment is also present in analogous benzamide derivatives showing interatomic H...O distances in the range 2.3–2.5 Å.⁸

In the two molecules of **5a** the distances between H-3' and O-1 are 2.410 and 2.399 Å, while in **7a** the analogous distance H-3'...O-3 is 2.34 Å. This arrangement causes the convexity of the boat to be oriented towards O-1 in both the molecules of **5a** and towards O-3 in **7a** (Table 2).

It is interesting to compare the conformation of the tropane of our compounds with those found in the crystal structures of analogous 5-HT₃ antagonists. An extensive search in the Cambridge Crystallographic Data Centre⁹ showed only crystal structures in which the piperidine adopts a chair conformation. The X-ray structures of

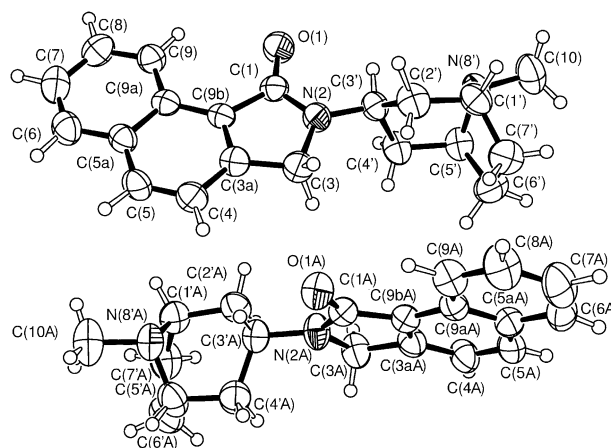


Figure 1. View of the two molecules of the asymmetric unit of **5a**. Ellipsoids enclose 50% probability.

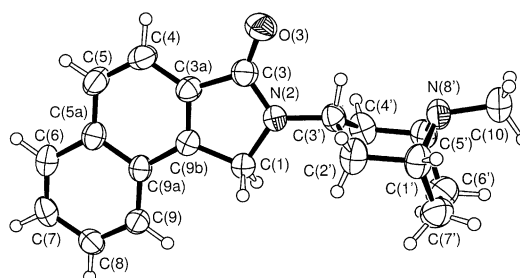


Figure 2. Crystal structure of compound **7a**. Ellipsoids enclose 50% probability.

5a and **7a** are profoundly different from them. In fact, in both derivatives, the piperidine ring of tropane moiety cannot adopt a chair conformation because of the transannular steric interactions of the tropane ethylene bridge hydrogens with the pyrrolidone moiety. This steric hindrance can be minimized by adopting a boat conformation without rotating the tropane residue around the bond N-2–C-3'. In fact, with the rotation of the tropane moiety, the interaction H-3'...O will be reduced or lost together with an ideal mirror plane in which the benzoisindolone moiety and C-3' and N-8' lie. It follows that in both structures the piperidine ring has a boat conformation as can be seen from the puckering parameters and torsion angles (Table 2). Finally, in both the crystal structures, the methyl group (C-10) is bound to N-8 in equatorial position. The crystal packing of both structures is stabilized by van der Waals interactions.

NMR spectroscopic studies. A complete assignment of ^1H NMR spectrum of compound **5a** was performed by the analysis of 2D-COSY and NOESY spectra carried out at 600 MHz. Table 3 summarizes the complete assignment of ^1H NMR signals of compound **5a**.

The key information afforded by the NOESY spectrum was the cross-peak between methylene C-3 protons and the higher field couple of H-2'/H-4' (2'/4'pa protons, see Table 3). Moreover, H-3' was connected by dipolar coupling only to the lower field couple of H-2'/H-4' (2'/4'pe protons, see Table 3), and the cross-peak between 2'/4'pe and 1'-5' protons was bigger than that between 2'/4'pa and 1'-5' protons. These results were consistent with the assignment of the higher field H-2'/H-4' signal to the axial protons in the piperidine boat conformation typical of the crystal structure. However, the appearance of a quintet-like signal at 4.67 ppm (H-3') was not consistent with the piperidine boat conformation; therefore, a comparative study between the experimental coupling constants and those calculated for different conformations of the tropane moiety was undertaken.

A reliable determination of the coupling constant was achieved by performing 2D J -resolved experiments at 600 MHz and extensive simulations of monodimensional and bidimensional ^1H NMR spectra (COSY). Table 3 reports the experimental coupling constant

values obtained from these studies and those calculated (MacroModel 5.0)¹⁰ for three different conformations of the tropane moiety.

When compared with **5a**, desmethyl derivative **5b** and quaternary derivative **5c** showed differences in the mono-dimensional ^1H NMR signals attributable to the tropane moiety and quite similar COSY and NOESY connections. These observations allowed an easy assignment of the ^1H NMR signals of **5b** and **5c** and suggest that different coupling constants (and different conformational preferences) should be involved. Compound **5b** showed the signal attributable to 3' proton as an apparent nonet at 4.58 ppm (the splitting pattern is compatible with a coupling with two protons with a J value of about 12 Hz and with other two protons with a J value of about 8 Hz), the signal attributable to 2'/4'pe protons as an apparent doublet of triplets at 2.38 ppm (from which the J values of about 13, 8 and 8 Hz can be abstracted), and the signal attributable to 2'/4'pa protons as an apparent triplet at 1.51 ppm (the splitting pattern is compatible with the coupling J values of about 13 and 12 Hz).

Quaternary derivative **5c** showed the signal attributable to 3' proton as an apparent triplet at 4.83 ppm (from which the J value of about 10 Hz can be abstracted), the signal attributable to 2'/4'pe protons as an apparent septet at 2.78 ppm (the splitting pattern is compatible with the coupling J values of about 14, 10 and 6 Hz), and the signal attributable to 2'/4'pa protons as a doublet at 2.18 ppm from which the J value of about 14 Hz can be abstracted.

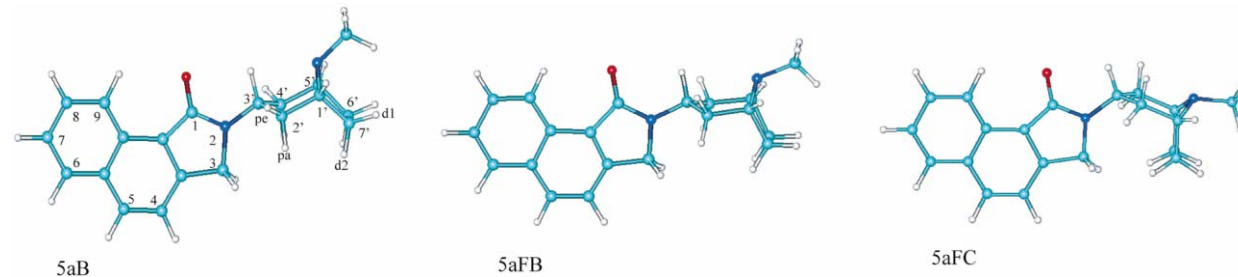
Conformational preferences. The comparison between the experimental J values and those calculated (MacroModel 5.0) for three different conformations of the tropane moiety (Table 3) suggests that (in solution) the tropane piperidine ring of **5a** adopts a conformation intermediate (conformation **5aFB** in Table 3) between the boat (conformation **5aB** in Table 3) and the flattened chair (conformation **5aFC** in Table 3) ones. Alternatively, it may show a rapid inversion between these two limit forms.

By way of comparison, nortropane derivative **5b** shows experimental J values similar to those calculated for the

Table 2. Torsion and puckering parameters of **5a** and **7a**

Torsion angle (°)	5a (mol. 1)	5a (mol. 2)	7a		
C(3')-C(4')-C(5')-N(8')	-19.01	-11.41	-13.16		
N(8')-C(1')-C(2')-C(3')	14.08	16.76	17.76		
N(2)-C(3')-C(4')-C(5')	-167.43	-174.85	-173.86		
C(1)-N(2)-C(3')-N(8')	-158.61	7.81	168.31		
C(1)-N(2)-C(3')-C(2')	130.76	127.51	-59.93		
C(2')-C(1')-N(8')-C(10)	166.09	167.07	162.70		
Compd	q2 (Å)	q3 (Å)	ϕ (°)	Θ (°)	Puckering amplitude (Å)
5a (mol. 1)	0.834	0.160	79.2	357.56	0.849
5a (mol. 2)	0.855	0.135	81.1	357.86	0.866
7a	0.843	0.147	80.1	1.85	0.856

Puckering parameters of the ring C(1')-C(2')-C(3')-C(4')-C(5')-N(8) (according to ref 27).

Table 3. ^1H NMR (600 MHz) characteristics of compound **5a**. Comparison of the experimental coupling constant (J) values with those calculated for three different conformations of **5a**


H	No.	δ (ppm)	Apparent moltep.	COSY contacts	Exp. J (Hz)	H Involv. in the coupl.	Theor. J Hz			NOESY contacts
							5aB	5aFB	5aFC	
1'-5'	2	3.3	m (5)	2'-4'pe	8.2 (3J)	2'-4'pe (3J)	9.5	7.8	5.3	2'-4'pe
				6'-7'd1	4.0 (3J)	2'-4'pa (3J)	2.2	1.1	1.9	2'-4'pa
					4.0 (4J)	7'-6'd1 (3J)	8	7.5	8.2	6'-7'd1
						6'-7'd1 (4J)				
						6'-7'd2 (3J)	1.3	1.2	1.3	
2'-4'pe	2	2.54	m (6)	2'-4'pa	14.0 (2J)	2'-4'pa (2J)				CH ₃
				1'-5'	8.2 (3J)	1'-5' (3J)	9.5	7.8	5.3	2'-4'pa
2'-4'pa	2	1.62	m (4)	3'	8.2 (3J)	3' (3J)	4.9	7.9	9.3	1'-5'
				2'-4'pe	14.0 (2J)	2'-4'pe (2J)				3'
				3'	8.2 (3J)	1'-5' (3J)	2.2	1.1	1.9	2'-4'pe
						3' (3J)	11.2	8.7	1.8	1'-5'
3'	1	4.67	m (5)	2'-4'pe	8.2 (3J)	2'-4'pe (3J)	4.9	7.9	9.3	3
				2'-4'pa	8.2 (3J)	2'-4'pa (3J)	11.2	8.7	1.8	2'-4'pe
6'-7'd1	2	2.21	m (7)	6'-7'd2	12.0 (2J)	6'-7'd2 (2J)				6'-7'd2
					4.0 (3J)	7'-6'd2 (3J)	3.8	3.9	3.8	
				1'-5'	4.0 (3J)	5'-1' (3J)	8	7.5	8	1'-5'
					4.0 (4J)	1'-5' (4J)				
6'-7'd2	2	1.66	m (4)	6'-7'd1	12.0 (2J)	6'-7'd1 (2J)				6'-7'd1
					4.0 (3J)	7'-6'd1 (3J)	3.8	3.9	3.8	
						5'-1' (3J)	1.3	1.2	1.3	
CH ₃	3	2.27	s (1)							1'-5'
3	2	4.43	s (1)							2'-4'pa
4	1	7.51	d (2)	5	8.3					4
5	1	7.99	d (2)	4	8.3					5
6	1	7.92	d (2)	7	8.1					3
7	1	7.57	m (7)	6	8.1					4
				8	Not determ.					7
8	1	7.66	m (7)	7	Not determ.					6
				9	8.5					8
9	1	9.27	d (2)	8	8.5					7

boat conformation of **5a** (conformation **5aB** in Table 3), while **5c** shows experimental J values close to those calculated for the flattened chair conformation of the tropane piperidine ring (conformation **5aFC** in Table 3). Indeed, in the latter compound the additional methyl group on the tropane nitrogen atom constrains the piperidine ring in the flattened chair conformation as suggested by the computational studies.

In summary, the conformational preferences of the tropane piperidine ring of these compounds appear to be affected by the substituent(s) present on the tropane nitrogen atom. In particular, the presence of a hydrogen atom stabilizes the boat conformation, while in the presence of a methyl group a rapid interconversion between the boat and the flattened chair conformation occurs,

and the presence of two methyl group constrains the tropane piperidine ring in the flattened chair conformation. A relationship is likely to exist between the oscillation of the piperidine ring from one of the two limit forms to the other and the pyramidal inversion of the tropane nitrogen atom. In fact, in compound **5a** the pyramidal inversion (the methyl group passing from the equatorial to the axial position) would be impossible without the oscillation of the piperidine ring.

Finally, the NOESY cross-peak between methylene C-3 and 2'/4'pa protons suggests the existence (also in solution) of a conformational preference at the level of the rotation around the tropane moiety single bond attachment to the fused pyrrolidone nucleus, which is also shown by crystallography.

Discussion

The interactions at the central 5-HT₃ receptor

The most interesting result emerging from the SAFIR studies is that the quaternization of the basic nitrogen of almost all the tropane and quinuclidine derivatives studied lowers their 5-HT₃ receptor affinity as observed for arylpiperazine derivatives.^{4c,6e,g} The only clear exception is represented by dimethyl quaternary tropane derivative **5c**, which shows an affinity indistinguishable from that shown by the corresponding monomethyl derivative **5a**. It is noteworthy that quaternization of the basic nitrogen of tropisetron, which shows a geometry of heteroarylcarbonyl backbone related to that of **5c** and **5a**, gave similar results.^{6a} Moreover, the effects of the quaternization of the basic nitrogen of these 5-HT₃ receptor ligands appear to be strictly structure-dependent. For example, in the small subclass of tropane ligands they seem to be affected by the geometry of the heteroaromatic moiety, while in the case of the quinuclidine derivatives studied both the configuration at the chiral center and the structural features of the heteroaromatic moiety may play a role.

These results fully agree with the assumption that different binding modes are operative at 5-HT₃ receptor binding site.^{5,11} In particular, from a mechanistic point of view, they suggest that a positive charge delocalized in the proximity of the basic nitrogen is important in the preliminary step of receptor recognition (long range interaction); then the subsequent step of ligand docking into the binding site(s) is driven by the structural features of the heteroaromatic moiety in such a way as to maximize the complementarity between the ligand and the binding site(s). In other words, the orientation of the ligands into its binding domain is mainly controlled by the short-range and directional interactions (dispersion interactions and H-bond interactions), while the positive charge establishing a strong, but long-range non-directional interaction with a suitable counterpart plays a relatively minor role in the docking step. Thus, the different effects of the quaternization of the basic nitrogen may reflect the differences in the amino acid environment sampled by the positively-charged group.

The identical affinity showed by tropane derivatives **5a**, **5b**, and **5c** appears to be intriguing because, from the point of view of the interaction with the receptor, these compounds show identical heteroaromatic portions, but they are quite dissimilar in the moiety containing the charged nitrogen. In fact, in nortropane derivative **5b** it bears two hydrogen atoms, in **5a** a methyl group and a hydrogen atom, and in quaternary derivative **5c** two methyl groups. Thus, the protonated nitrogen atom of **5a** and **5b** can (in principle) establish a charge-assisted hydrogen bond with a negatively charged carboxylic amino acid residue in the receptor, while for quaternary derivative **5c** a purely ionic interaction is conceivable. Furthermore, the detailed structural study performed on these tropane derivatives revealed quite different conformational preferences (and consequently molecular dynamics) of the moiety bearing the basic nitrogen. In fact, the tropane piperidine ring is locked in the flat-

tened chair conformation in quaternary derivative **5c**, while in **5b** and **5a** a rapid interconversion between the boat and the flattened chair conformation occurs (with a higher stability of the boat conformation in compound **5b**). On the whole, the substituent(s) on the basic nitrogen affects both the possibility of interaction with the receptor counterpart and the conformational preferences in the key moiety, but not the affinity for the receptor. These observations could lead to the assumption that the interaction of the charged nitrogen is, in any case, purely ionic.¹² However, the assumption appears to oversimplify the problem since it does not take into account all the potential interactions that the charged nitrogen and its substituents can establish in the interaction with the receptor and the possible existence of multiple compensatory effects.

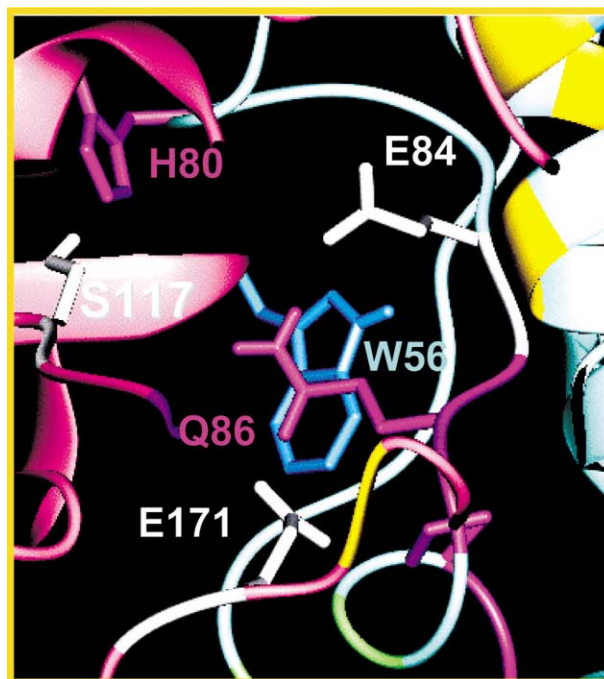


Figure 3. Residues participating to the inter-subunit network of hydrogen bonds formed in the isolated receptor during dynamics.

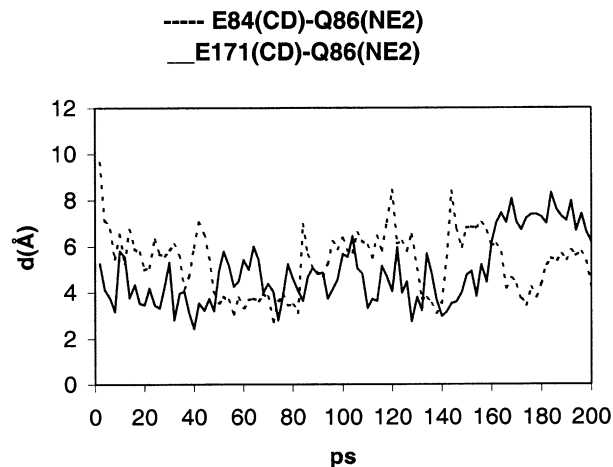


Figure 4. Time evolution of the distances between the Q86 side chain nitrogen (NE2, in CHARMM parameter file) and the E84 (dotted line), or E171 (solid line) carboxylic carbon atom (CD).

In the light of all these considerations, the rationalization of the SAFIR data was attempted by means of docking experiments.

Molecular simulations of the isolated receptor show that an inter-subunit network of hydrogen bonding is formed during dynamics (Fig. 3). It concerns mainly

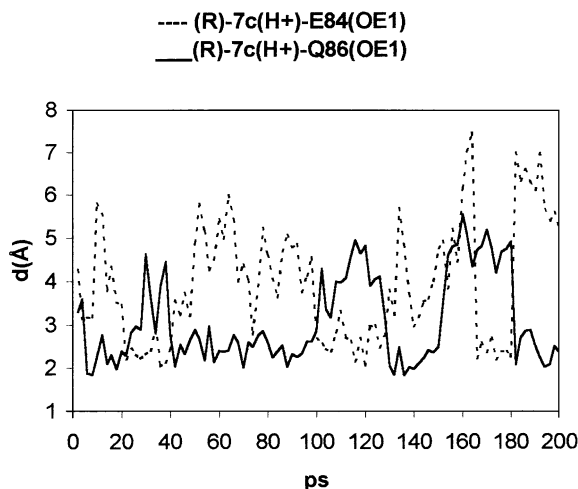


Figure 5. Time evolution of the distances between the E84 side chain oxygen atom (OE1, in CHARMM parameter file) and the Q86 (dotted line) and the side chain oxygen atom (OE1) and the full agonist (*R*)-7c cationic head (solid line).

amino acids which have proved to be important for the conformational equilibrium and ligand binding in the 5-HT₃ subtypes and/or in members of the LGIC receptor family. The glutamine 86 (Q86, belonging to the second subunit) establishes a dynamic bridge between the glutamic acid E171 (first subunit) and E84 (second subunit). W56 of the first subunit makes a hydrogen bond with the carbonyl oxygen of the second subunit E84 backbone. Moreover, a hydrogen bond between the S117 (first subunit) and H80 (second subunit) is observed. The persistence of the interactions involving Q86 during dynamics is shown in Figure 4, where the distances between the Q86 side chain nitrogen (NE2, in CHARMM parameter file) and the E84, or E171 carboxylic carbon atom (CD) are plotted.

The binding paradigm proposed in our previous papers^{5,11} suggests that this network is perturbed in a different way when the ligand is bound, depending on its functional phenotype. Accordingly, antagonists **5a** and (*S*)-**5d** establish a charge-assisted hydrogen bonding interaction between their positively charged head and the negatively charged carboxylic tail of E171 (first receptor subunit), while full agonist (*R*)-**7c** binds E84 (second receptor subunit). The analysis of the trajectories of the molecular dynamics simulation study supports this hypothesis. Moreover, it shows that Q86 participates in (or competes with E84 for) this interaction (Fig. 5). Partial agonist (*R*)-**5d** shares the same

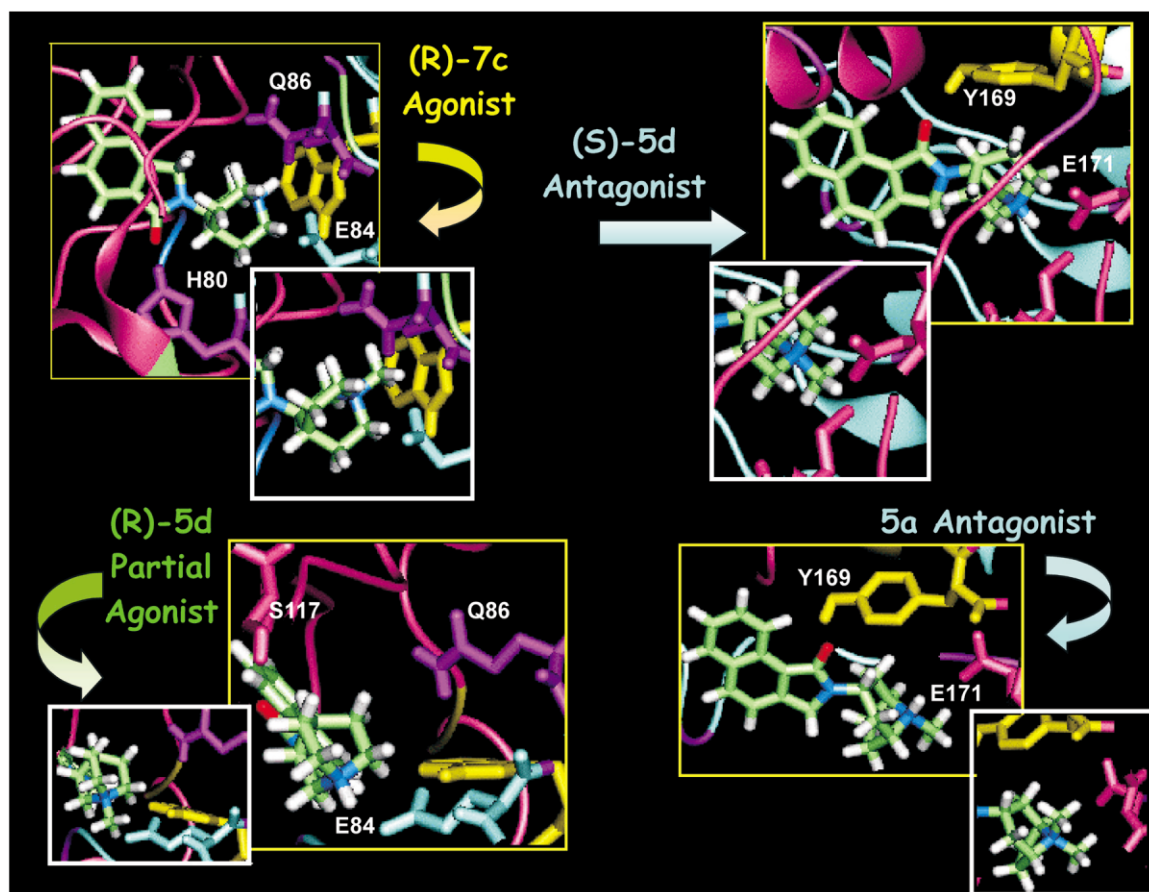


Figure 6. Details of the binding interactions for the agonist (*R*)-**7c**, the partial agonist (*R*)-**5d**, the antagonists (*S*)-**5d** and **5a**, and their quaternary analogues.

main interaction with E84, but Q86 is not involved in the binding. The second pharmacophoric element, the carbonyl oxygen atom in the heteroaromatic moiety, establishes an hydrogen bonding interaction with Y169 (first receptor subunit), or H80 in its protonated state (second receptor subunit) and S117 (first receptor subunit) according to the antagonist, agonist or partial agonist activities. Finally, specific (π – π) interactions between the ligand aromatic moiety and F104 and/or F158, and short range dispersion interactions between ligand substituents and I55, L99 and/or L119 are observed.

The importance of the hydrogen bond interaction between the protonated nitrogen of the ligands which show agonist activity and Q86 seems to be confirmed by the experimental finding of 100-fold drop in the affinity of the quaternary analogue of (*R*)-**7c**. In fact, as is shown in Figure 6, the quaternary analogue is able to accommodate in the same binding pocket, but the only optimized interaction is with W25. According to the binding paradigm previously proposed, the partial agonist (*R*)-**5d** does not interact with Q86, in full agreement with the fact that its quaternization does not affect binding significantly. In fact, the binding site is not significantly perturbed by the methylation of compound (*R*)-**5d** (Fig. 6).

An extensive comparison of the results of the molecular dynamics simulations carried out both on the protonated and quaternary antagonists suggests that methylation of the quinuclidine derivatives causes a large rearrangement of the receptor first subunit loop comprised between amino acids 55 and 67, in order to avoid steric hindrance with I62. This might contribute to the significant loss of affinity [from 59 to 80 times for compounds (*S*)-**5d** and (*S*)-**7c**, respectively] upon quaternization.

On the contrary, the binding affinity of the antagonist **5a** is not affected by quaternization, as is also shown by the minimized average structure of the complex (Fig. 6).

Conclusions

With the aim of exploring the effects of the quaternization of the ligand basic nitrogen on the 5-HT₃ receptor affinity systematically, we have (a) selected several representatives from a new class of potent 5-HT₃ receptor ligands containing either the tropane or quinuclidine moieties **5–7**, (b) quaternized their basic nitrogen atoms by reaction with methyl iodide, (c) studied their structure and conformational preferences by means of X-ray, NMR, and molecular modeling techniques, (d) measured their binding affinity, and (e) rationalized the results with the help of three-dimensional ligand-receptor models derived by Molecular Dynamics studies.

This study reveals that the effects of the quaternization of the basic nitrogen of these 5-HT₃ receptor ligands are strictly structure-dependent supporting the hypothesis that different binding modes are operative at 5-HT₃ receptor binding site. In fact, the orientation of the ligands within their binding domains appears to be controlled

mainly by the short-range and directional interactions (dispersion interactions and H-bond interactions), while the positive charge, establishing a strong, but long-range non-directional interaction with a suitable counterpart, plays a relatively minor role in the docking step. Therefore, the different effects of the quaternization of the basic nitrogen reflect the differences in the amino acid environment sampled by the positively-charged group or, from another perspective, the different efficacy of the binding reorganization induced by the additional methyl group of the quaternary derivatives.

Experimental

Chemistry

Melting points were determined in open capillaries on a Gallenkamp apparatus and are uncorrected. Microanalyses were carried out by means of a Perkin-Elmer 240C or a Perkin-Elmer Series II CHNS/O Analyzer 2400. Merck silica gel 60 (70–230 or 230–400 mesh) and Merck aluminumoxid 90 II-III, 70–230 mesh were used for column chromatography. Merck TLC plates, silica gel 60 F₂₅₄ were used for TLC. ¹H NMR spectra were recorded with a Bruker AC 200 and Bruker DRX 600 spectrometers in the indicated solvents (TMS as internal standard): the values of chemical shifts are expressed in ppm and coupling constants (*J*) in Hz. Mass spectra were recorded on a VG 70–250S spectrometer.

General procedure for the synthesis of target quaternary derivatives **5c,e**, **6b,d,f**, and **7b,d**

A mixture of the appropriate free base (**5a,d**, **6a,c,e**, and **7a,c**)⁵ (0.1 mmol) in 5 mL of methanol with methyl iodide (0.25 mL, 4.0 mmol) was stirred at room temperature under argon for a suitable time (3 days for tropane derivatives **5a**, **6a**, and **7a** and 1 h for quinuclidine derivatives **5d**, **6c,e**, and **7c**). The volatile was removed under reduced pressure and the residue was washed with diethyl ether or ethyl acetate, and dried to give the expected quaternary derivative (**5c,e**, **6b,d,f**, and **7b,d**).

endo-2-(8,8-Dimethyl-8-azoniabicyclo[3.2.1]oct-3-yl)-2,3-dihydro-1H-benz[e]isoindol-1-one iodide (5c**).** The title compound was prepared from free base **5a** and was purified by washing with diethyl ether (yield 83%, mp 265–267 °C dec). ¹H NMR (200 MHz, DMSO-*d*₆): 2.09–2.46 (m, 6H), 2.78 (m, 2H), 3.01 (s, 3H), 3.14 (s, 3H), 3.88 (br s, 2H), 4.76 (s, 2H), 4.83 (t, *J* = 10.0, 1H), 7.54–7.74 (m, 3H), 8.04 (d, *J* = 7.9, 1H), 8.15 (d, *J* = 8.4, 1H), 9.03 (d, *J* = 7.9, 1H); (600 MHz, DMSO-*d*₆): 2.17 (d, *J* = 14.0, 2H, 2'/4'pa), 2.26 (m, 2H, 6'/7'd2), 2.44 (m, 2H, 6'/7'd1), 2.79 (m, 2H, 2'/4'pe), 3.07 (s, 3H, CH₃), 3.18 (s, 3H, CH₃), 3.92 (br s, 2H, 1'/5'), 4.78 (s, 2H, 3), 4.83 (t, *J* = 10.4, 1H, 3'), 7.59 (m, 1H, 7), 7.69 (m, 1H, 8), 7.73 (m, 1H, 4), 8.06 (d, *J* = 8.1, 1H, 6), 8.17 (d, *J* = 8.3, 1H, 5), 9.05 (d, *J* = 8.3, 1H, 9). MS(FAB): *m/z* 321 (C₂₁H₂₅N₂O⁺, 100). Anal. (C₂₁H₂₅IN₂O·0.25H₂O) C, H, N.

endo-2-(8,8-Dimethyl-8-azoniabicyclo[3.2.1]oct-3-yl)-2,3-dihydro-1H-benz[e]isoindol-1-one iodide (6b**).** The title

compound was prepared from free base **6a** and was purified by washing with ethyl acetate (yield 79%, mp 298–300 °C dec). ¹H NMR (200 MHz, DMSO-*d*₆): 2.11–2.47 (m, 6H), 2.78 (m, 2H), 3.01 (s, 3H), 3.14 (s, 3H), 3.89 (br s, 2H), 4.79–4.88 (m, 3H), 7.54–7.65 (m, 2H), 8.01–8.13 (m, 3H), 8.29 (s, 1H). Anal. (C₂₁H₂₅IN₂O·0.5H₂O) C, H, N.

endo-2-(8,8-Dimethyl-8-azoniabicyclo[3.2.1]oct-3-yl)-1,2-dihydro-3H-benz[e]isoindol-3-one iodide (7b). The title compound was prepared from free base **7a** and was purified by washing with ethyl acetate (yield 78%, mp 276–278 °C dec). ¹H NMR (200 MHz, DMSO-*d*₆): 2.19–2.46 (m, 6H), 2.78 (m, 2H), 3.02 (s, 3H), 3.15 (s, 3H), 3.90 (br s, 2H), 4.76 (t, *J* = 9.9, 1H), 5.03 (s, 2H), 7.64–7.70 (m, 3H), 8.00 (d, *J* = 8.5, 1H), 8.04–8.09 (m, 1H), 8.15–8.19 (m, 1H). Anal. (C₂₁H₂₅IN₂O·0.5H₂O) C, H, N.

2-(1-Methyl-1-azoniabicyclo[2.2.2]oct-3-yl)-2,3-dihydro-1H-benz[e]isoindol-1-one iodide (5e). The enantiomers of compound **5e** were prepared from enantiomerically pure free base (*S*)-**5d** and (*R*)-**5d** and were purified by washing with diethyl ether. ¹H NMR (200 MHz, CDCl₃–DMSO-*d*₆ 5:1): 1.85–2.39 (m, 5H), 3.14 (s, 3H), 3.43–3.62 (m, 2H), 3.68–3.82 (m, 1H), 4.08 (m, 2H), 4.47–4.67 (m, 3H), 4.76 (d, *J* = 17.8, 1H), 7.41–7.54 (m, 3H), 7.80 (d, *J* = 8.4, 1H), 7.90 (d, *J* = 8.5, 1H), 8.92 (d, *J* = 7.6, 1H).

(*S*)-**5e**: yield 84%; mp 184–186 °C dec. Anal. (C₂₀H₂₃IN₂O·0.25H₂O) C, H, N.

(*R*)-**5e**: yield 87%; mp 183–185 °C dec. Anal. (C₂₀H₂₃IN₂O·0.5H₂O) C, H, N.

2-(1-Methyl-1-azoniabicyclo[2.2.2]oct-3-yl)-2,3-dihydro-1H-benz[f]isoindol-1-one iodide (6d). The enantiomers of compound **6d** were prepared from enantiomerically pure free base (*S*)-**6c** and (*R*)-**6c** and were purified by washing with diethyl ether. ¹H NMR (200 MHz, CDCl₃–DMSO-*d*₆ 5:1): 1.70–2.17 (m, 4H), 2.32 (m, 1H), 2.98 (s, 3H), 3.33–3.62 (m, 3H), 3.88 (m, 2H), 4.25–4.34 (m, 1H), 4.39–4.53 (m, 2H), 4.71 (d, *J* = 16.1, 1H), 7.26–7.38 (m, 2H), 7.65–7.77 (m, 3H), 8.03 (s, 1H).

(*S*)-**6d**: yield 78%; mp 297–298 °C. Anal. (C₂₀H₂₃IN₂O·2.5H₂O) C, H, N.

(*R*)-**6d**: yield 82%; mp 299–301 °C. Anal. (C₂₀H₂₃IN₂O·0.5H₂O) C, H, N.

2-(1-Methyl-1-azoniabicyclo[2.2.2]oct-3-yl)-2,3-dihydro-1H-pyrrolo[3,4-*b*]quinolin-1-one iodide (6f). The enantiomers of compound **6f** were prepared from enantiomerically pure free base (*S*)-**6e** and (*R*)-**6e** and were purified by washing with diethyl ether. ¹H NMR (200 MHz, DMSO-*d*₆): 1.83–2.32 (m, 4H), 2.37 (m, 1H), 3.00 (s, 3H), 3.48 (m, 4H), 3.86 (m, 2H), 4.63 (t, *J* = 8.2, 1H), 4.87 (q, *J* = 16.8, 2H), 7.68 (t, *J* = 7.3, 1H), 7.89 (t, *J* = 7.3, 1H), 8.10 (d, *J* = 8.5, 1H), 8.21 (d, *J* = 8.0, 1H), 8.80 (s, 1H).

(*S*)-**6f**: yield 89%; mp > 300 °C dec. Anal. (C₁₉H₂₂IN₃O·H₂O) C, H, N.

(*R*)-**6f**: yield 93%; mp > 300 °C. Anal. (C₁₉H₂₂IN₃O·2H₂O) C, H, N.

2-(1-Methyl-1-azoniabicyclo[2.2.2]oct-3-yl)-1,2-dihydro-3H-benz[e]isoindol-3-one iodide (7d). The enantiomers of compound **7d** were prepared from enantiomerically pure free base (*S*)-**7c** and (*R*)-**7c** and were purified by washing with diethyl ether. ¹H NMR (200 MHz, CDCl₃–DMSO-*d*₆ 5:1): 2.00–2.48 (m, 4H), 2.56 (m, 1H), 3.19 (s, 3H), 3.63 (m, 3H), 4.08 (m, 2H), 4.51 (m, 1H), 4.65 (m, 1H), 5.03 (q, *J* = 17.7, 2H), 7.57 (m, 2H), 7.68 (d, *J* = 8.2, 1H), 7.84–8.00 (m, 3H).

(*S*)-**7d**: yield 84%; mp 257–259 °C. Anal. (C₂₀H₂₃IN₂O·H₂O) C, H, N.

(*R*)-**7d**: yield 81%; mp 258–260 °C. Anal. (C₂₀H₂₃IN₂O·0.25H₂O) C, H, N.

In vitro binding assays

Binding assays were performed as described in ref 7. Male Wistar rats (Charles River, Calco, Italy) were killed by decapitation and their brains were rapidly removed at 4 °C, and cortex and hippocampus were dissected out. Tissues were homogenized (Polytron PTA 10TS) in ice-cold Hepes buffer, 50 mM, pH 7.4, and centrifuged according to the procedures indicated in the above-cited reference. The pellet obtained was finally suspended in Hepes buffer 50 mM, pH 7.4, just before the binding assay was performed. [³H]Granisetron (s.a. 81 Ci/mmol; NEN Life Science Products) binding were assayed in final incubation volumes of 1.0 mL. Tissue and [³H]ligand final concentrations were: 20 mg of tissue/sample and 0.5 nM, respectively. The specific binding of the tritiated ligands was defined as the difference between the binding in the absence (total binding) and in the presence of 100 μM unlabeled 5-HT (non-specific binding). It represented in an average 70% of the total binding.

Incubation was interrupted by rapid filtration under vacuum through Whatman GF/B glass fiber filters pre-soaked in Hepes buffer 50 mM, pH 7.4, containing 0.1% polyethyleneimine. Filters were immediately rinsed with 12 mL (3×4 mL) of ice-cold buffer by means of a Brandel M-24R cell harvester, dried and immersed into vials containing 8 mL of Ultima Gold MV (Packard Biosciences) for the measurement of trapped radioactivity with a TRI-CARB 1900TR (Packard Biosciences) liquid scintillation spectrometer, at a counting efficiency of about 60%. Competition experiments were analyzed by the 'Allfit' program¹³ to obtain the concentration of unlabelled drug that caused 50% inhibition of [³H]granisetron specific binding (IC₅₀). Apparent affinity constants (*K*_i) were derived from the IC₅₀ values according to the Cheng and Prusoff equation.¹⁴ The *K*_d value for [³H]granisetron specific binding calculated from saturation isotherms was found to be 0.6 nM.

X-Ray crystallography

Single crystals of **5a**, and **7a**, were submitted to X-ray data collection on a Siemens P4 four-circle diffractometer

with graphite monochromated Mo- K_{α} radiation ($\lambda=0.71069$ Å). The $\omega/2\theta$ scan technique was used. The structures were solved by direct methods and the refinements were carried out by full-matrix anisotropic least-squares of F^2 against all reflections. The hydrogen atoms were located on Fourier difference maps and included in the structure-factor calculations with a common isotropic temperature factor. Atomic scattering factors including f' and f'' were taken from ref 15. Structure solution and refinement were carried out by using the SHELX-97 package¹⁵ while molecular graphics was performed by the WINGX program.¹⁶

5a. $C_{20}H_{22}N_2O$ (MW 306.4), a single crystal, colorless needle, dimensions $0.6 \times 0.2 \times 0.2$ mm, was used for data collection; monoclinic; space group $P2_1/c$ (n. 14); $a=10.785(2)$, $b=13.315(2)$, $c=23.045(3)$ Å, $\beta=98.18(1)^\circ$, $V=3275.6(9)$ Å³, $Z=8$, $D_c=1.24$ g/cm³. A total of 5758 unique reflections ($R_{\text{int}}=0.027$) were collected at 22 °C. The final refinement converged to $R=0.056$ and $wR_2=0.099$ for $F^2 > 2\sigma(I)$. Minimum and maximum heights in last $\Delta\rho$ map were -0.19 and 0.17 eÅ⁻³.

7a. $C_{20}H_{22}N_2O$ (MW 306.4), a single crystal, colorless prism, dimensions $0.4 \times 0.4 \times 0.2$ mm, was used for data collection; monoclinic; space group $P2_1/c$ (n. 14); $a=14.433(2)$, $b=12.476(2)$, $c=9.673(1)$ Å, $\beta=107.77(1)^\circ$, $V=1658.7(4)$ Å³, $Z=4$, $D_c=1.23$ g/cm³. A total of 2930 unique reflections ($R_{\text{int}}=0.048$) were collected at 22 °C. The final refinement converged to $R=0.050$ and $wR_2=0.096$ for $F^2 > 2\sigma(I)$. Minimum and maximum heights in last $\Delta\rho$ map were -0.17 and 0.15 eÅ⁻³.

Crystallographic data (with the exception structure factors) for the structures in this paper have been deposited with the Cambridge Crystallographic Data Centre as supplementary publication nos. CCDC175503 (**7a**), CCDC175504 (**5a**). Copies of the data can be obtained, free of charge, on application to CCDC, 12 Union Road, Cambridge CB2 1EZ, UK (fax: +44-1223-336033 or e-mail: deposit@ccdc.cam.ac.uk).

NMR

1D- and 2D-NMR experiments were performed on a Bruker DRX-600 AVANCE spectrometer operating at 600.13 MHz and 150.89 MHz for ¹H and ¹³C respectively, equipped with an xyz gradient unit. A reverse triple resonance (¹H, ¹³C, BB) probe with xyz gradients was used.

2D J -resolved spectra¹⁷ were acquired using a spectral width of 80 Hz along F1 and 2048 and 128 data points in F2 and F1 respectively.

NOESY¹⁸ and dqf-COSY¹⁹ were acquired with 2048 complex points for 256 experiments with 6 s recycle delay and TPPI²⁰ phase cycle. A 45° shifted squared-sine window function was applied to both dimensions for every set of data and zero filled to 1024 points along F1.

NOESY sets of spectra were acquired with mixing times of 50, 200 and 600 ms.

The data was processed with NMRpipe²¹ (version 3.3) software, and 2D spectra were analyzed with SPARKY software.²² Integration of the cross-peak volumes in the NOESY spectrum was done by means of the Gaussian-fitting algorithm of SPARKY.

Computational methods

The structures of all compounds studied were fully optimized by means of molecular orbital calculation, using the MOPAC 6.0 (QCPE 455) program. The three-dimensional structure of ligands **5a** and **7a** solved by X-ray crystallography in our laboratory (see text), were taken as input for AM1 optimization.²³ The starting geometries of the other derivatives considered were constructed by means of the Cerius2 program.²⁴

Ligands **5a**, **5c**, **5d** (*R,S*), **5e** (*R,S*), **7c** (*R,S*), and **7d** (*R,S*) were manually docked in the minimized average structure of the receptor previously published,¹¹ by satisfying the binding modalities of the ligands according to their functionalities.

The complexes were energy minimized by means of the program CHARMM.²⁵ The minimization procedure consisted of 50 steps of steepest descent, followed by a conjugate gradient minimization until the rms gradient of the potential energy was less than 0.001 kcal/mol Å. The united atom force-field parameters, a 12 Å non-bonded cutoff and a dielectric constant $\epsilon=4r$ were used.

The minimized coordinates of the complexes were used as starting point for dynamics. During dynamics the lengths of the bonds involving hydrogen atoms were constrained according to the SHAKE algorithm,²⁶ allowing an integration time step of 0.001 picoseconds (ps). The β -sheet structure was maintained by means of the NOE utility provided by the CHARMM program, which allows the imposition of constraints between atoms belonging to opposite strands.

The structures were thermalized to 300 K with 5 °C rise per 6000 steps by randomly assigning individual velocities from the Gaussian distribution. After heating, the systems were allowed to equilibrate until the potential energy versus time was approximately stable (34 ps). Velocities were scaled by a single factor. An additional 10 ps period of equilibration with no external perturbation was run. Time-averaged structures were then determined over the last 200 ps of each simulation. Data were collected every 0.5 ps.

Acknowledgements

Thanks are due to the Italian MURST for financial support. Prof. Stefania D'Agata D'Ottavi's careful reading of the manuscript is also acknowledged. Unlabeled granisetron was a generous gift of Smith Kline Beecham Pharmaceuticals.

References and Notes

1. Jackson, M. B.; Yakel, J. L. *Annu. Rev. Physiol.* **1995**, *57*, 447.
2. Boess, F. G.; Martin, I. L. *Neuropharmacology* **1994**, *33*, 275.
3. Silverstone, P. H.; Greenshaw, A. J. *Exp. Opin. Ther. Pat.* **1996**, *6*, 471.
4. (a) Anzini, M.; Cappelli, A.; Vomero, S.; Giorgi, G.; Langer, T.; Hamon, M.; Merahi, N.; Emerit, B. M.; Cagnotto, A.; Skorupska, M.; Mennini, T.; Pinto, J. C. *J. Med. Chem.* **1995**, *38*, 2692. (b) Cappelli, A.; Donati, A.; Anzini, M.; Vomero, S.; De Benedetti, P. G.; Menziani, M. C.; Langer, T. *Bioorg. Med. Chem.* **1996**, *4*, 1255. (c) Cappelli, A.; Anzini, M.; Vomero, S.; Mennuni, L.; Makovec, F.; Doucet, E.; Hamon, M.; Bruni, G.; Romeo, M. R.; Menziani, M. C.; De Benedetti, P. G.; Langer, T. *J. Med. Chem.* **1998**, *41*, 728. (d) Cappelli, A.; Anzini, M.; Vomero, S.; Canullo, L.; Mennuni, L.; Makovec, F.; Doucet, E.; Hamon, M.; Menziani, M. C.; De Benedetti, P. G.; Bruni, G.; Romeo, M. R.; Giorgi, G.; Donati, A. *J. Med. Chem.* **1999**, *42*, 1556.
5. Cappelli, A.; Anzini, M.; Vomero, S.; Mennuni, L.; Makovec, F.; Doucet, E.; Hamon, M.; Menziani, M. C.; De Benedetti, P. G.; Giorgi, G.; Ghelardini, C.; Collina, S. *Bioorg. Med. Chem.* **2002**, *10*, 779.
6. (a) Watling, K. J.; Aspley, S.; Swain, C. J.; Saunders, J. *Eur. J. Pharmacol.* **1988**, *149*, 397. (b) Dukat, M.; Miller, K.; Teitler, M.; Glennon, R. A. *Med. Chem. Res.* **1991**, *1*, 271. (c) Swain, C. J.; Baker, R.; Kneen, C.; Moseley, J.; Saunders, J.; Seward, E. M.; Stevenson, G.; Beer, M.; Stanton, J.; Watling, K. *J. Med. Chem.* **1991**, *34*, 140. (d) Swain, C. J.; Baker, R.; Kneen, C.; Herbert, R.; Moseley, J.; Saunders, J.; Seward, E. M.; Stevenson, G. I.; Beer, M.; Stanton, J.; Watling, K.; Ball, R. G. *J. Med. Chem.* **1992**, *35*, 1019. (e) Anzini, M.; Cappelli, A.; Vomero, S.; Cagnotto, A.; Skorupska, M. *Med. Chem. Res.* **1993**, *3*, 44. (f) Langlois, M.; Soulier, J. L.; Mathé-Allainmat, M.; Gallais, C.; Brémont, B.; Shen, S. *Bioorg. Med. Chem. Lett.* **1994**, *4*, 945. (g) Rault, S.; Lancelot, J. C.; Prunier, H.; Robba, M.; Renard, P.; Delagrangé, P.; Pfeiffer, B.; Caignard, D. H.; Guardiola-Lemaitre, B.; Hamon, M. *J. Med. Chem.* **1996**, *39*, 2068.
7. Nelson, D. R.; Thomas, D. R. *Biochem. Pharmacol.* **1989**, *38*, 1693.
8. (a) Collin, S.; Moureau, F.; Quintero, M. G.; Vercauteren, D. P.; Evrard, G.; Durant, F. *J. Chem. Soc., Perkin Trans. 2* **1995**, *77*. (b) Bradley, G.; Ward, T. J.; White, J. C.; Coleman, J.; Taylor, A.; Rhodes, K. F. *J. Med. Chem.* **1992**, *35*, 1515.
9. Cambridge Crystallographic Data Centre (CCDC) 12 Union Road, Cambridge CB2 1EZ, UK.
10. *Macromodel 5.0*; Columbia University: New York, 1995.
11. Menziani, M. C.; De Rienzo, F.; Cappelli, A.; Anzini, M.; De Benedetti, P. G. *Theor. Chem. Acc.* **2001**, *106*, 98.
12. Gaster, L. M.; King, F. D. *Med. Res. Rev.* **1997**, *17*, 163.
13. De Lean, K. W.; Munson, P. J.; Rodbard, D. *Am. J. Physiol.* **1978**, *235*, E97.
14. Cheng, Y.; Prusoff, W. H. *Biochem. Pharmacol.* **1973**, *22*, 3099.
15. Sheldrick, G. M. *SHELX-97, Rel. 97–2, Program for X-ray Data Diffraction*; Göttingen University, 1997.
16. Farrugia, L. J. *J. Appl. Cryst.* **1999**, *32*, 837.
17. Aue, W. P.; Karhan, J. M.; Ernst, R. R. *J. Chem. Phys.* **1976**, *64*, 4226.
18. Macura, S.; Wüthrich, K.; Ernst, R. R. *J. Magn. Reson.* **1982**, *46*, 269.
19. Piantini, U.; Sorensen, O. W.; Ernst, R. R. *J. Am. Chem. Soc.* **1982**, *104*, 6800.
20. Bodenhausen, G.; Freeman, R.; Morris, G. *J. Magn. Reson.* **1976**, *23*, 171.
21. Delaglio, F.; Grzesiek, S.; Vuister, G.; Zhu, G.; Pfeifer, J.; Bax, A. *J. Biomol. NMR* **1995**, *6*, 277.
22. *SPARKY Program for NMR Assignment and Integration*; Computer Graphics Laboratory, University of California, San Francisco, USA, 2000.
23. Dewar, M. J. S.; Zoebisch, E. G.; Healey, E. F.; Stewart, J. J. P. *J. Am. Chem. Soc.* **1985**, *107*, 3902.
24. *Cerius2*; Molecular Simulations; San Diego, 1997.
25. Brooks, B. R.; Bruccoleri, R. E.; Olafson, B. D.; States, D. J.; Swaminathan, S.; Karplus, M. *J. Comput. Chem.* **1983**, *4*, 187.
26. van Gunsteren, W. F.; Berendsen, J. C. *Mol. Phys.* **1977**, *34*, 1311.
27. Cremer, D.; Pople, J. A. *J. Amer. Chem. Soc.* **1975**, *97*, 1354.